A Substrate Channel in Nitrogenase Revealed by a Molecular Dynamics Approach

ARTICLE *in* BIOCHEMISTRY · MARCH 2014

Impact Factor: 3.02 · DOI: 10.1021/bi401313j · Source: PubMed

4 AUTHORS, INCLUDING:

Dayle M A Smith
Pacific Northwest National Laboratory
38 PUBLICATIONS **818** CITATIONS
SEE PROFILE

Simone Raugei
Pacific Northwest National Laboratory
96 PUBLICATIONS **1,742** CITATIONS
SEE PROFILE

Lance Seefeldt
Utah State University
136 PUBLICATIONS **5,388** CITATIONS
SEE PROFILE

BIOCHEMISTRY
including biophysical chemistry & molecular biology

Article

pubs.acs.org/biochemistry

Substrate Channel in Nitrogenase Revealed by a Molecular Dynamics Approach

Dayle Smith,*[,†] Karamatullah Danyal,[‡] Simone Raugei,[†] and Lance C. Seefeldt*[,‡]

[†]Pacific Northwestern National Laboratory, Richland, Washington 99352, United States

[‡]Department of Chemistry and Biochemistry, Utah State University, Logan, Utah 84322, United States

Supporting Information

ABSTRACT: Mo-dependent nitrogenase catalyzes the biological reduction of N_2 to two NH_3 molecules at FeMo-cofactor buried deep inside the MoFe protein. Access of substrates, such as N_2, to the active site is likely restricted by the surrounding protein, requiring substrate channels that lead from the surface to the active site. Earlier studies on crystallographic structures of the MoFe protein have suggested three putative substrate channels. Here, we have utilized submicrosecond atomistic molecular dynamics simulations to allow the nitrogenase MoFe protein to explore its conformational space in an aqueous solution at physiological ionic strength, revealing a putative substrate channel. The viability of this observed channel was tested by examining the free energy of passage of N_2 from the surface through the channel to FeMo-cofactor, resulting in the discovery of a very low energy barrier. These studies point to a viable substrate channel in nitrogenase that appears during thermal motions of the protein in an aqueous environment and that approaches a face of FeMo-cofactor earlier implicated in substrate binding.

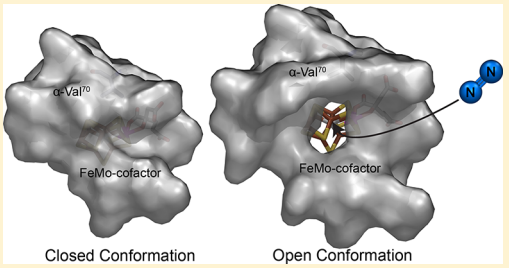

Mo-dependent nitrogenase, the most prevalent of the nitrogenase enzymes, catalyzes the reduction of N_2 to two NH_3 molecules, with an optimal reaction stoichiometry shown in eq 1.[1,2]

$$N_2 + 8e^- + 16MgATP + 8H^+ \rightarrow 2NH_3 + H_2 + 16MgADP + 16Pi \quad (1)$$

The nitrogenase complex is composed of the Fe protein and the MoFe protein.[1] The Fe protein contains a single [4Fe−4S] cluster and two adenosine triphosphate (ATP) binding sites.[3] It functions to deliver electrons to the MoFe protein, one at a time, during the transient association of the two proteins with the coupled hydrolysis of the two ATP molecules to two adenosine diphosphate (ADP) and two phosphate (P_i).[1,4−6] The heterotetrameric MoFe protein ($\alpha_2\beta_2$) houses two different types of metal clusters. The [8Fe−7S] P cluster is located near the Fe protein binding interface and is proposed to function as an electron carrier between the Fe protein and the active site [7Fe−9S−1Mo−C−*R*-homocitrate] FeMo-cofactor contained within the MoFe protein.[7−11] FeMo-cofactor is buried deep (15.5 Å below surface) within each α subunit of the MoFe protein. Although the known substrates for nitrogenase are relatively small molecules (e.g., N_2, C_2H_2),[1,12,13] it has been proposed that access of these substrates to the active site is highly restricted by the surrounding protein matrix.[7,8,14,15] Such restrictive access of small molecules to the buried active site of several other metalloenzymes has been validated through calculations and experimentation.[16−20]

Earlier studies on nitrogenase that explored possible substrate channels from the surface of the MoFe protein to the active-site FeMo-cofactor have utilized structures derived from X-ray crystal studies.[7,16,17,21] Three putative channels have been proposed from such studies, starting from MoFe protein surface residues β-513^{Gln}, α-106^{Val}, or α-104^{Thr}.[16−18,22] Although different methods were used to identify the putative channels in these studies, all utilized static protein structures. A separate proton relay system starting at α-281^{Tyr} on the surface was proposed as a possible pathway for proton delivery to FeMo-cofactor.[17] In one of the studies, amino acid substitutions were made in the proposed channel, and the effects on substrate reduction rates were examined.[16] The results were consistent with the conclusion that the proposed pathway functioned to control access of some substrates to the active site.

Protein structures are dynamic, and the range of motions experienced by a protein might impact substrate channels. For some proteins, substrate channels may be apparent only during thermal motion in a physiological environment. To explore this possibility for the nitrogenase enzyme, we have applied submicrosecond molecular dynamics simulations to the MoFe protein of nitrogenase, allowing the protein to equilibrate under ambient conditions in an aqueous environment under realistic ionic strength conditions. Similar simulations, in conjunction with experimental measurements, have proven to be valuable in understanding gas transport in other metalloproteins, such as O_2 and H_2 diffusion through enzymes.[23−25] We have found that a putative substrate channel within the MoFe protein is revealed that was not apparent in the crystallographic structure.

Received: September 20, 2013
Revised: March 6, 2014

   dx.doi.org/10.1021/bi401313j | *Biochemistry* XXXX, XXX, XXX−XXX

To test the viability of this channel, the thermodynamics for the translocation of a N_2 molecule from the surface to the active-site FeMo-cofactor through the channel is reported.

METHODS

Model Building. Starting coordinates were taken from a 1.0 Å resolution X-ray structure of MoFe protein from *Azotobacter vinelandii* (Protein Data Bank ID 3U7Q).[10] The MoFe protein ($\alpha_2\beta_2$ tetramer) contains 52 histidine residues, 26 in each $\alpha\beta$ dimer. The protonation state of the histidines was determined using PropKa[26] and visual inspection. On the basis of this analysis, histidines 80 and 195 of chains A and C (α1 and α2) and histidines 193, 311, 363, 392, 396, and 429 of chains B and D (β1 and β2) were protonated at Nε, histidines 90 and 359 of chains A and C were protonated at both Nδ and Nε, and the rest were protonated at Nδ. The initial structure contains two calcium ions, two magnesium ions, and 2602 embedded water molecules that were included in the model. The protein was inserted into a rectangular box filled with water molecules ($162 \times 131 \times 118$ Å^3), which was based on a minimum clearance of 15 Å between solute atoms and the sides of the box. To neutralize the system and to model experimentally realistic solvent conditions, 273 sodium ions and 227 chloride ions were added by replacing bulk solvent atoms to achieve 0.15 M ionic strength (the embedded water molecules from the initial X-ray diffraction structure were not replaced with ions). The total number of atoms is 253 357.

Potential Energy Function Setup. Knowledge of the potential energy term for each atom is a prerequisite to classical molecular simulations. We used the AMBER03 force field to describe the protein potential energy terms[27] and the TIP3P model for water molecules,[28] and we derived parameters for the [8Fe−7S] and [7Fe−9S−Mo−C] clusters and attached ligands (homocitrate, cysteinates, and the Mo-bound histidine). Model metal clusters representative of the resting state were built by truncating protein ligands at Cα and replacing them with a hydrogen atom. Equilibrium bond lengths and angles for the metal clusters and immediately attached groups were taken from the initial structure, and stiff bond (k_r) and angle (k_a) force constants were used to maintain the initial atomic configuration (k_r = 500 kcal mol^{-1} Å^{-2}, k_a = 200 kcal mol^{-1} rad^{-2}). Metal cluster dihedrals were not included in the model. Bond, angle, and dihedral parameters for homocitrate were derived using the generalized AMBER force field (GAFF).[29] Atom-centered charges were calculated by restrained electrostatic potential fitting (RESP)[30] to DFT (density functional theory) electrostatic potentials using the BLYP DFT functional, the 6-31G* basis on all C, N, O, S, and H atoms, and a double-ζ basis set on metal ions.[31] The resulting atom-centered charges and additional charge-fitting details are included in the Supporting Information. Nickel and iron Lennard−Jones parameters were taken from Smith et al.,[32] and unknown Mo Lennard−Jones parameters were copied from Ni (which is a reasonable approximation because the Mo ion is coordinated to six atoms: sulfur atoms, homocitrate, and protein histidine). The nitrogen substrate (N_2) is a neutral, linear, symmetrical molecule with a permanent quadrupole moment. The quadrupole moment was modeled with three point charges arranged along the N−N bond, two on the N atoms, and one on the center of mass of the molecule. The potential parameters for the N_2 potential were taken from ref 33.

Equilibration and Molecular Dynamics. All classical simulations were done using GROMACS 4.5.5 programs.[34] The solvated structure of nitrogenase was energy-minimized to a maximum atomic force tolerance of 24 kcal mol^{-1} Å^{-1}, and this energy-minimized structure was used as the starting structure for equilibration. All equilibration molecular dynamics simulations were done at constant temperature (300 K) and pressure (1 atm) maintained using a modified Berendsen thermostat and barostat.[35] The system was gradually heated to 300 K by performing fifteen 250 ps long consecutive simulations. In the first simulation, non-hydrogen atoms were restrained using harmonic position restraints with a force constant of 2.4 kcal mol^{-1} Å^{-2}, and the temperature was set at 100 K. In the next four steps, the temperature was increased in 50 K increments to 300 K. Then, restraint forces were gradually reduced to zero in 10 consecutive runs. The system was then let free to evolve for 100 ns with temperature and pressure maintained with the Nosé−Hoover thermostat[36] and Parrinello−Rahman barostat.[37] All of the simulations were carried out using an integration time step for the equations of motion of 2 fs, and all of the bonds involving H atoms were kept fixed.[38]

Trajectory Analyses. To assess convergence of atomic fluctuations and to examine backbone and side-chain movements relevant to substrate penetration, the following trajectory analyses were performed: (1) thermal-averaged atom-to-atom root-mean-squared deviation (rmsd) from the initial structure as a function of time for protein backbone atoms after superimposing backbone atoms; (2) normal-mode analysis based on covariance analysis of backbone atoms displacements; (3) minimum distance between selected groups of atoms along the channel as a function of time; (4) analysis of channel-lining residues using the Hollow1.2 Python program[39] (0.02 Å grid spacing and 1.4 Å probe radius); and (5) structure visualization and trajectory animation using Visual Molecular Dynamics (VMD 1.9.1).[40] The rmsd stabilizes after 20 ns (Figure S1) and consequently all properties were calculated averaging on the trajectory segment from 20 to 100 ns.

Free Energy for N_2 Uptake. Umbrella sampling simulations[41] were performed to assess the thermodynamic feasibility of N_2 insertion into the observed channel deduced from the molecular dynamics trajectory. The free energy for the N_2 uptake was calculated along distance, r, between the FeMo-cofactor central carbide atom and the center of mass of the surface protein residues at the channel entrance. Transient contacts between these residues can influence substrate access and consequently the energetics for N_2 could be biased by the selected initial configuration. For this reason, two different simulations were performed starting from configurations extracted from the molecular dynamics trajectory. In one configuration (referred to hereafter as open), the surface residues are separated (defined by the closest distance between residues), and in the other (the closed configuration), the surface residues are in close proximity. To generate initial umbrella sampling window configurations (N_2 positions along the channel), continuous pulling calculations were done for each initial configuration (open and closed) by placing the N_2 substrate 25 Å from the FeMo-cofactor central carbide and pulling the N_2 toward the interstitial carbide (C) at a rate of 0.02 Å ps^{-1} using a harmonic biasing potential with a force constant of 12 kcal mol^{-1} Å^{-2}. The positions of the umbrella sampling windows were selected from these continuous pulling trajectories with C−N_2 distances of between 4 and 24 Å, with a 0.5 Å spacing between 4 and 12 Å and a 1.0 Å spacing between 12 and 24 Å, for a total of 29 umbrella sampling windows for each conformation (open and closed). Umbrella sampling molecular

dx.doi.org/10.1021/bi401313j | *Biochemistry* XXXX, XXX, XXX−XXX

dynamics calculations were conducted for each configuration using a harmonic constraint potential relative to each initial spring position and a force constant of 2.4 kcal mol^{-1} $Å^{-2}$. Following 500 ps of equilibration, statistics were collected for 2 ns, corresponding to a total of 58 ns for each initial conformation. The final free-energy profile (potential of mean force, PMF) was calculated using statistical analysis of the spring positions with the weighted histogram analysis method.[41] Errors were calculated using 200 bootstraps,[42] and the final 1D PMF plots were Jacobian-corrected by adding the customary $2k_BT\ \ln(r)$ term.[43] It is important to point out that the concentration of N_2 in the equilibrated simulation cell (6×10^{-4} M) corresponds to the N_2 concentration in water under ambient conditions when the solution is saturated with air. Therefore, the calculated free energy for N_2 uptake corresponds exactly to free energy under ambient conditions, and no additional correction for concentration is needed.

RESULTS

Molecular Dynamics Simulations. Protein structures are highly dynamic, and thermal fluctuations of amino acid residues might modulate the access to core regions, disclosing access channels not discernible from the analysis of crystallographic structures. To examine this possibility in nitrogenase, we applied long-time-scale (submicrosecond) molecular dynamics simulations to the MoFe protein under realistic conditions (0.15 M ionic strength at ambient pressure and temperature). General structural properties of the solvated MoFe protein and convergence of the protein fluctuations are first discussed. Upon solvation and equilibration, the thermal-averaged backbone atom-to-atom distance from the initial crystal structure stabilizes to the value rmsd = 1.9 ± 0.1 Å after 20 ns of simulation (Supporting Information Figure S1), a value in line with typical values obtained from MD simulations and solution NMR spectroscopy of globular proteins in aqueous solution. The major differences between the protein structure in solution and the initial structure are found in the unstructured regions (loops) and chain-terminal residues (illustrated in Supporting Information Figure S2). Also consistent with typical results from MD simulations, there is a 6% increase of the solvent-exposed surface with respect to the X-ray structure, which is indicative of slight protein expansion in solution. Covariance analysis[44] (see the Supporting Information) shows that the simulation is long enough to sample the relevant long-time-scale structural fluctuations of the MoFe protein about the equilibrium. Taken together, there is high confidence that the force field and the overall simulation protocol are appropriate to capture thermally induced conformational dynamics of the MoFe protein.

Appearance of a Possible Substrate Channel. The side chains of α-281^{Tyr}, α-277^{Arg}, and α-383^{His} are observed to undergo significant movement during relaxation, creating a possible channel connecting FeMo-cofactor to the surface of the protein. The side chain of α-281^{Tyr} is close to the polar side chains of α-277^{Arg} (1.9 Å) and α-383^{His} (3.8 Å) in the crystal structure (Figure 1), with α-277^{Arg} situated between α-281^{Tyr} and α-383^{His}. During the protein expansion in the first 10 ns of simulation at 300 K, the spacing between the surface residues α-281^{Tyr} and α-383^{His} increases and allows α-277^{Arg} to rotate toward FeMo-cofactor and to form a hydrogen bond with it (with a distance of 3.33 ± 0.58 Å between Arg(Nη1) and FeMo-cofactor S1A), illustrated in Figure 2. In fact, α-277^{Arg} has previously been proposed to form a surface "flap" controlling substrate access to the cofactor.[7] As expected for residues located on the surface of a protein, the side chains of α-281^{Tyr} and α-383^{His} exhibit large-amplitude fluctuations and dynamically alternate between closed and open structures (Figures 1 and 2). Figure 2 shows the closest distance between α-281^{Tyr} and α-383^{His} as a function of time for the $\alpha_1\beta_1$ and $\alpha_2\beta_2$ holoproteins. On the time scale of our simulation, the channel in the $\alpha_1\beta_1$ unit alternates between a closed and open

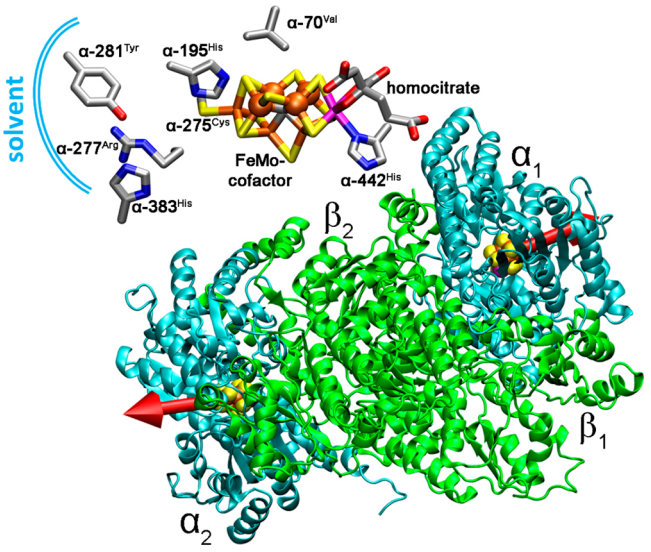

Figure 1. Key residues near the channel entrance and FeMo-cofactor in the initial crystal structure. The solvent is to the left of FeMo-cofactor, showing the position of α-277^{Arg}, α-281^{Tyr}, and α-383^{His} side chains, which are hydrogen bonded in the initial crystal structure (top). α-275^{Cys} and α-442^{His} residues are shown coordinated with FeMo-cofactor, whereas the α-195^{His} and α-70^{Val} residues are shown to highlight the relevant face of FeMo-cofactor. The nitrogenase protein structure viewed from the same perspective is also shown (bottom), with the substrate channel indicated with red arrows directed from FeMo-cofactor. The protein is represented as a ribbon (cyan for α1 and α2 and green for β1 and β2), and carbon is shown in gray, oxygen, in red, sulfur, in yellow, iron, in rust, and molybdenum, in magenta.

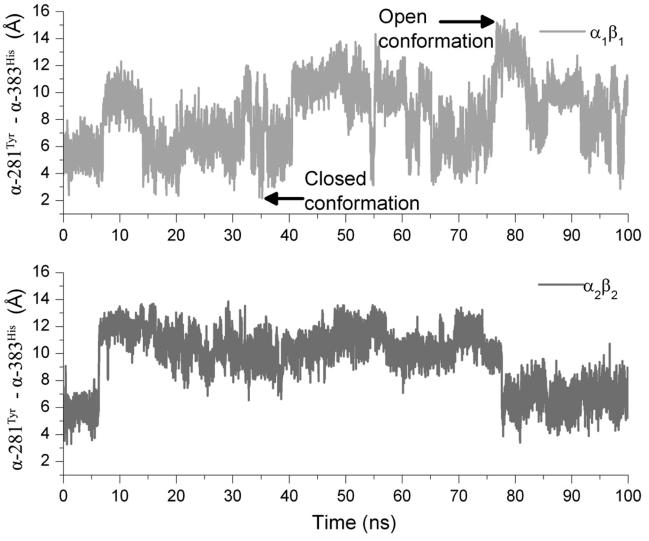

Figure 2. Fluctuation of the distance between residues α-281^{Tyr} and α-383^{His}. The closest distance between α-281^{Tyr} and α-383^{His} is plotted as a function of time. Top panel, $\alpha_1\beta_1$ unit; bottom panel, $\alpha_2\beta_2$ unit. Open and closed conformations are noted.

dx.doi.org/10.1021/bi401313j | Biochemistry XXXX, XXX, XXX−XXX

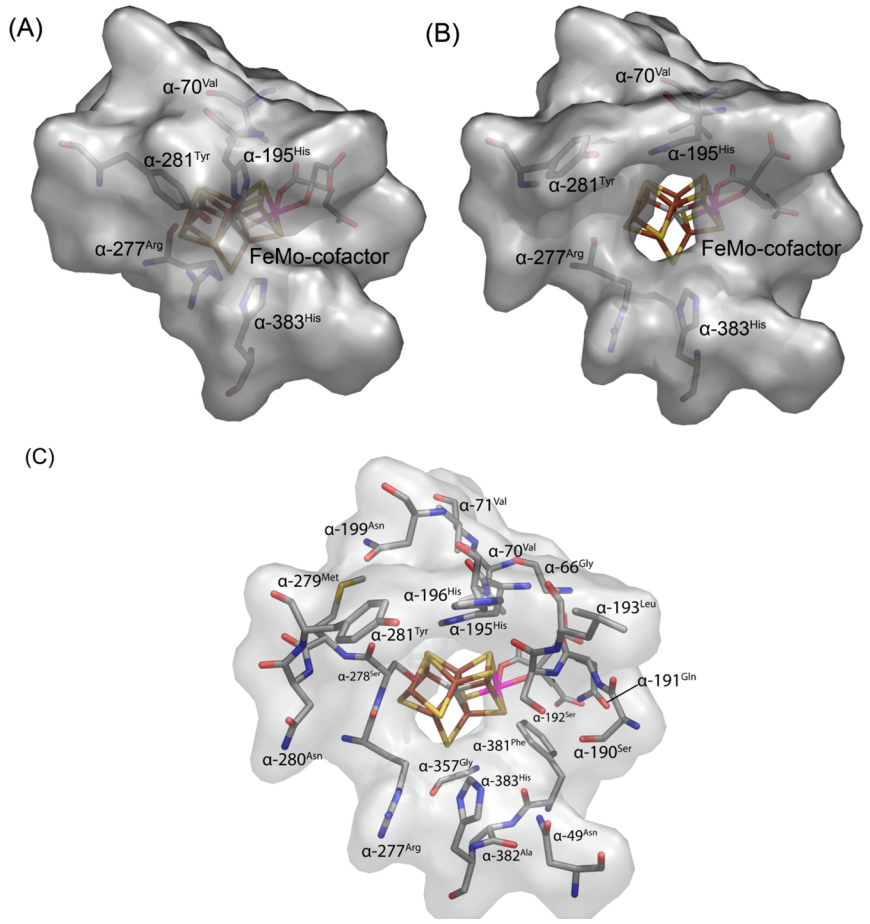

Figure 3. Surface representation of the proposed channel. Protein surface (A) in the starting x-ray structure and (B) in the open conformation at 76 ns. Both panels show surface representation of the 20 residues that constitute the channel, with α-70^{Val}, α-195^{His}, α-281^{Tyr}, α-277^{Arg}, and α-383^{His} residues shown in stick representation as well. (C) Transparent surface representation to highlight the channel in which all 20 residues of the channel are shown in stick representation.

configuration more frequently than in the $\alpha_2\beta_2$ unit. In both units, the minimum and maximum distances between the gating residues α-281^{Tyr} and α-383^{His} are similar (4 and 14 Å, respectively). A surface representation of the initial x-ray structure and open channel structure after simulation is reported in Figure 3.

N_2 Substrate Access Channel. The average nitrogenase structure was used for channel analysis using the Hollow program.[39] In the average structure, the channel entrance is open. Although α-195^{His} Hε is hydrogen-bonded to FeMo-cofactor S2B in the initial structure, this residue is actually quite flexible and can also bind to S2A. In the average structure, α-195^{His} Hε is closest to S2A (2.6 Å), leaving S2B more exposed. There are 20 protein residues lining the channel between FeMo-cofactor and α-281^{Tyr}/α-383^{His} from the Hollow analysis shown in Figure 3C: α-49^{Asn}, α-66^{Gly}, α-70^{Val}, α-71^{Val}, α-190^{Ser}, α-191^{Gln}, α-192^{Ser}, α-193^{Leu}, α-195^{His}, α-196^{His}, α-199^{Asn}, α-277^{Arg}, α-278^{Ser}, α-279^{Met}, α-280^{Asn}, α-281^{Tyr}, α-357^{Gly}, α-381^{Phe}, α-382^{Ala}, and α-383^{His}. The channel is shown in Figure 4A as a solute-excluded grid between FeMo-cofactor and α-281^{Tyr}/α-383^{His}.

This path leads to the proposed reactive face of FeMo-cofactor, which is composed of the iron atoms Fe2, Fe3, Fe6, and Fe7 (Figure 4). Importantly, residue α-70^{Val}, which has been shown to be important in substrate access to the catalytic core,[45−49] is part of this channel. These observations provide further support to the possible role of the channel disclosed by the molecular dynamics simulation in substrate passage to the active site.

Free Energy for N_2 Insertion. The energetics for N_2 insertion was evaluated for both the closed and open channel structures. Figure 5 shows the free-energy change for N_2 movement along the putative channel. In the open configuration, N_2 passes past α-281^{Tyr}/α-383^{His} unhindered. In the closed conformation, N_2 first encounters α-281^{Tyr}, and it is stabilized there by about 1 kcal mol^{-1}. However, it can move easily past α-281^{Tyr} and α-383^{His} (with a free-energy cost of only about 1.5 kcal mol^{-1}) and then continue along the same path as in the open conformation toward FeMo-cofactor. Once N_2 comes within 10 Å of FeMo-cofactor (defined by the distance to the central carbide ion), it moves into a vacant space near S2B (r = 6 Å). The barrier holding N_2 in place is only 0.8 ± 0.6 kcal mol^{-1}. Starting from the r = 6 Å umbrella sampling window in the open conformation, N_2 was let free to explore accessible states around this position for 2 ns. As expected on the basis of the barrier and the available thermal energy, N_2 crosses the small barrier discussed above and moves toward the entrance of the channel after a relatively short time (800 ps) (Figure S3). However, in this short time, N_2 explores a relatively large portion of space around FeMo-cofactor on the side of the channel (Figure 6). The simulation revealed preferential interactions of N_2 and α-His^{195}, α-192^{Ser}, and the

dx.doi.org/10.1021/bi401313j | Biochemistry XXXX, XXX, XXX−XXX

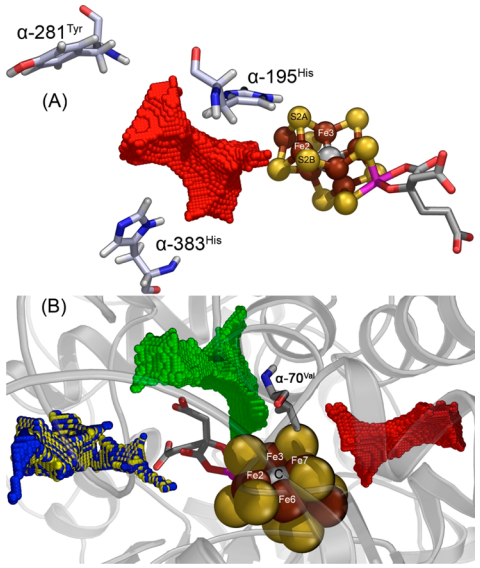

Figure 4. Substrate access channels. (A) Side-on-view (solvent to the left) of the proposed substrate access channel calculated using Hollow by superimposing the nitrogenase structure in the open conformation onto a 3D grid with 0.02 Å spacing between grid points. Unoccupied grid points are represented by red spheres. (B) Positions of the channel proposed here (red spheres) and the channels proposed by Barney[16] (green spheres), Dance[18] (yellow spheres), and Durrant[17] (blue spheres). Carbon is shown in gray, oxygen, in red, hydrogen, in white, sulfur, in yellow, iron, in rust, and molybdenum, in magenta.

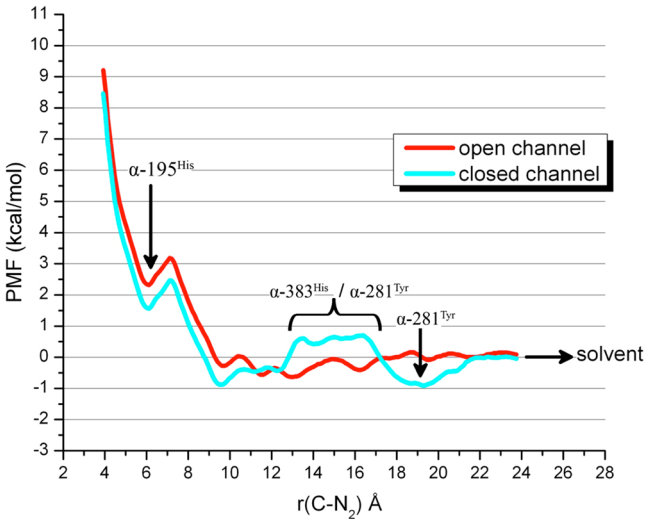

Figure 5. Free energy for the N_2 insertion from solvent to FeMo-cofactor along the proposed channel in unit $\alpha_1\beta_1$ as a function of the distance between the N_2 center of mass and the carbide at the center of FeMo-cofactor. Starting conformations were taken from molecular dynamics snapshots corresponding to the open (76 ns) (red) and closed (36 ns) (cyan) channels. Graphs including error bars are shown in Supporting Information Figure S3.

S2B sulfur atom of FeMo-cofactor. During this simulation time, N_2 is also able to explore the space around iron atom Fe6 that has been proposed to bind N_2.

The simulations revealed that although α-His^{195} Hε is hydrogen-bonded to FeMo-cofactor S2B in the initial structure, this residue is actually quite flexible and can also bind to S2A. In both initial conformations, α-His^{195} Hε is closer to S2A than to S2B; the Hε-S2A and Hε-S2B distances are 3.4 and 5.1 Å in the

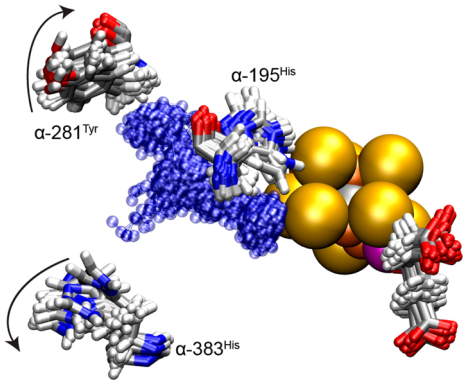

Figure 6. Structures from a molecular dynamics simulation of free N_2 in solvated nitrogenase. Ten superimposed structures from a 2 ns trajectory (200 ps snapshots). FeMo-cofactor and N_2 (blue spheres) are represented as van der Waals spheres, whereas amino acid residues and *R*-homocitrate are represented as sticks. Carbon is shown in gray, oxygen, in red, hydrogen, in white, sulfur, in yellow, iron, in rust, molybdenum, in magenta, and N_2, in blue.

open conformation and 2.6 and 3.9 Å in the closed conformation, leaving S2B more exposed.

In summary, the free-energy calculations show that the proposed channel allows for easy access to FeMo-cofactor in both the closed and open states. The overall activation free energy under ambient conditions is 3.2 and 2.5 kcal mol^{-1} for the two states, respectively. As a consequence of the high flexibility of the protein residues near the cavity surface, there is a very low activation free energy near r = 15 Å, the point at which N_2 displaces α-281^{Tyr} and α-383^{His}.

DISCUSSION

By using explicit-solvent molecular dynamics simulations under physiological-like ionic strength and ambient temperature and pressure, we have observed side-chain fluctuations that open a putative substrate channel access to FeMo-cofactor that is not observable from the static crystal structures.[10,50,51] During the simulations, the nitrogenase backbone atoms maintained a conformation similar to the initial crystal structure, whereas side-chain fluctuations disclose a direct channel from the surface to a face of FeMo-cofactor that has been implicated in substrate binding.[2,52,53] The channel described here and proposed previously[7] is gated by molecular motions of the side chains of α-281^{Tyr} and α-383^{His}, which are hydrogen-bonded to each other in the crystal structure but are flexible during solution molecular dynamics. It was discovered that it takes a few tens of nanoseconds to fluctuate between minimum and maximum separation (the closed and open conformations, respectively, Figure 2) between these residues. The free-energy barrier of N_2 insertion from the center of mass of α-281^{Tyr} and α-383^{His} to FeMo-cofactor is small regardless of whether the insertion starts from the surface of the open or closed conformations (2.5 versus 3.2 kcal mol^{-1}, respectively), indicating that even when the surface residues are in closest contact the substrate can easily displace α-281^{Tyr} and α-383^{His} and access the channel proposed here.

The channel observed here following dynamic simulations can be compared to channels previously proposed (Figure 4B). Barney et al.,[16] analyzing crystallographic structures, proposed a water-based channel for substrate access that extends from solvent-exposed surface residue α-104^{Thr} to a water cavity near the *R*-homocitrate. The possible role of this putative channel

dx.doi.org/10.1021/bi401313j | *Biochemistry* XXXX, XXX, XXX−XXX

was experimentally tested by accessing the impact of amino acid substitutions at key locations in the proposed channel on substrate reduction rates. Single amino acid substitutions at four different amino acids within the channel located at a large distance from FeMo-cofactor caused significant increases in the Michaelis constant (K_m) for several substrates while not affecting the turnover number (k_{cat}). These findings were interpreted to favor this region of the MoFe protein acting as one channel for substrate access to the active site.[16]

Channels proposed by Durrant and Dance are roughly in the same location (Figure 4B).[17,18] An interstitial channel proposed by Durrant was observed in the crystal structures of the MoFe proteins from *Klebsiella pneumoniae* and *Azotobacter vinelandii*. Multiple structures of the MoFe protein were overlaid and studied for the presence of water molecules that might define a channel. The channel was found at the interstice between two subunits of the protein. Water molecules seemed to form a proton wire in the channel and provided access from the surface to a pool of water near homocitrate. A similar controlled relay of multiple protons was proposed by Dance via a water chain, with the destination for the proton wire being the S3B sulfur on FeMo-cofactor.

The present free-energy calculations suggest that the access of N_2 to FeMo-cofactor is very fast and therefore it is not rate-determining. As a consequence, it is unlikely that substitution of amino acids around the channel would result in detectable changes in turnover rates. An additional consideration is how the proposed channels approach FeMo-cofactor. A series of studies have provided compelling evidence that one FeS face of FeMo-cofactor approached by α-70^{Val} and α-195^{His} constitutes the initial binding site for a range of substrates.[2,49,53,54] The putative channel revealed here approaches one edge of the Fe 2, 3, 6, 7 face of FeMo-cofactor implicated in substrate binding, going past the critical side chains of α-70^{Val} and α-195^{His} (Figures 1 and 4B). The other two channels proposed by Barney[16] and Durrant/Dance[14,15,17,18] approach different edges of this FeMo-cofactor FeS face but do not pass by critical residues α-70^{Val} and α-195^{His} (Figure 4B).

Which of these channels is used by substrates to gain access to FeMo-cofactor? Studies to date do not allow a definitive answer to this question, but it certainly seems possible that more than one channel might be operative for different substrates, and it is possible that one of these channels might function as a path for egress of products away from the active site. Our free-energy calculations indicated that the channel proposed here offers a low-energy pathway for N_2 access to FeMo-cofactor. A recent computational study[55] suggests a possible channel for the product ammonia egress that is distinct from any of the putative channels discussed here. It will be interesting in subsequent studies to access the energy barriers for passage of other substrates and products through the channel highlighted here and through the other proposed channels.

■ ASSOCIATED CONTENT

Supporting Information

Convergence of sampling method; derived atom-centered charges; convergence of 100 ns molecular dynamics trajectory; average and initial nitrogenase structures; and one-dimensional potential of mean force for N_2 insertion for the proposed channel, including errors from bootstrap analysis. This material is available free of charge via the Internet at http://pubs.acs.org.

■ AUTHOR INFORMATION

Corresponding Authors

*(D.S.) E-mail: dayle.smith@pnl.gov; Phone: 509-375-4358; Fax: 509-371-7637.

*(L.C.S.) E-mail: lance.seefeldt@usu.edu; Phone: 435-797-3964; Fax: 435-797-3390.

Funding

This work was funded by the U.S. DOE Basic Energy Sciences (BES), Division of Chemical Sciences, Geosciences and Biosciences and DOE grant DE-SC0010687 (to L.C.S.). Computational resources were provided at W. R. Wiley Environmental Molecular Science Laboratory, Pacific Northwest National Laboratory.

Notes

The authors declare no competing financial interest.

■ ACKNOWLEDGMENTS

We thank Prof. Thomas C. Squier (Western University Health Sciences) for stimulating discussions.

■ ABBREVIATIONS USED

Fe protein, iron protein of nitrogenase; MoFe protein, molybdenum−iron protein of nitrogenase; FeMo-cofactor, iron−molybdenum cofactor; AMBER, Assisted Model Building with Energy Refinement; M cluster, iron−molybdenum cofactor; F cluster, [4Fe−4S] cluster of the Fe protein; P cluster, [8Fe−7S] cluster of the MoFe protein; rmsd, root-mean-square deviation; MD, molecular dynamics; DFT, density functional theory; PMF, potential of mean force

■ REFERENCES

(1) Burgess, B. K., and Lowe, D. J. (1996) Mechanism of molybdenum nitrogenase. *Chem. Rev. 96*, 2983−3012.

(2) Seefeldt, L. C., Hoffman, B. M., and Dean, D. R. (2009) Mechanism of Mo-dependent nitrogenase. *Annu. Rev. Biochem. 78*, 701−722.

(3) Georgiadis, M. M., Komiya, H., Chakrabarti, P., Woo, D., Kornuc, J. J., and Rees, D. C. (1992) Crystallographic structure of the nitrogenase iron protein from *Azotobacter vinelandii*. *Science 257*, 1653−1659.

(4) Hageman, R. V., Orme-Johnson, W. H., and Burris, R. H. (1980) Role of magnesium adenosine 5′-triphosphate in the hydrogen evolution reaction catalyzed by nitrogenase from *Azotobacter vinelandii*. *Biochemistry 19*, 2333−2342.

(5) Thorneley, R. N., Lowe, D. J., Eady, R. R., and Miller, R. W. (1979) The coupling of electron transfer in nitrogenase to the hydrolysis of magnesium adenosine triphosphate. *Biochem. Soc. Trans. 7*, 633−636.

(6) Lowe, D. J., Ashby, G. A., Brune, M., Knights, H., Webb, M. R., and Thorneley, R. N. F. (1995) ATP hydrolysis and energy transduction by nitrogenase, in *Nitrogen Fixation: Fundamentals and Applications* (Tikhonovich, I. A., Provorov, N. A., Romanov, V. I., and Newton, W. E., Eds.) pp 103−108, Kluwer Academic Publishers, Dordrecht, The Netherlands.

(7) Kim, J., and Rees, D. C. (1992) Structural models for the metal centers in the nitrogenase molybdenum-iron protein. *Science 257*, 1677−1682.

(8) Chan, M. K., Kim, J., and Rees, D. C. (1993) The nitrogenase FeMo-cofactor and P-cluster pair: 2.2 Å resolution structures. *Science 260*, 792−794.

(9) Lancaster, K. M., Roemelt, M., Ettenhuber, P., Hu, Y., Ribbe, M. W., Neese, F., Bergmann, U., and DeBeer, S. (2011) X-ray emission spectroscopy evidences a central carbon in the nitrogenase iron-molybdenum cofactor. *Science 334*, 974−977.

(10) Spatzal, T., Aksoyoglu, M., Zhang, L., Andrade, S. L. A., Schleicher, E., Weber, S., Rees, D. C., and Einsle, O. (2011) Evidence for interstitial carbon in nitrogenase FeMo cofactor. *Science 334*, 940.
(11) Einsle, O., Tezcan, F. A., Andrade, S. L. A., Schmid, B., Yoshida, M., Howard, J. B., and Rees, D. C. (2002) Nitrogenase MoFe-protein at 1.16 Å resolution: A central ligand in the FeMo-cofactor. *Science 297*, 1696−1700.
(12) Rivera-Ortiz, J. M., and Burris, R. H. (1975) Interactions among substrates and inhibitors of nitrogenase. *J. Bacteriol. 123*, 537−545.
(13) Seefeldt, L. C., Yang, Z.-Y., Duval, S., and Dean, D. R. (2013) Nitrogenase reduction of carbon-containing compounds. *Biochim. Biophys. Acta. 1827*, 1102−1111.
(14) Durrant, M. C. (2002) An atomic-level mechanism for molybdenum nitrogenase. Part 1. Reduction of dinitrogen. *Biochemistry 41*, 13934−13945.
(15) Durrant, M. C. (2002) An atomic-level mechanism for molybdenum nitrogenase. Part 2. Proton reduction, inhibition of dinitrogen reduction by dihydrogen, and the HD formation reaction. *Biochemistry 41*, 13946−13955.
(16) Barney, B. M., Yurth, M. G., Dos Santos, P. C., Dean, D. R., and Seefeldt, L. C. (2009) A substrate channel in the nitrogenase MoFe protein. *J. Biol. Inorg. Chem. 14*, 1015−1022.
(17) Durrant, M. C. (2001) Controlled protonation of iron-molybdenum cofactor by nitrogenase: A structural and theoretical analysis. *Biochem. J. 355*, 569−576.
(18) Dance, I. (2012) The controlled relay of multiple protons required at the active site of nitrogenase. *Dalton Trans. 41*, 7647−7659.
(19) Leroux, F., Dementin, S., Burlat, B., Cournac, L., Volbeda, A., Champ, S., Martin, L., Guigliarelli, B., Bertrand, P., Fontecilla-Camps, J., Rousset, M., and Léger, C. (2008) Experimental approaches to kinetics of gas diffusion in hydrogenase. *Proc. Natl. Acad. Sci. U.S.A. 105*, 11188−11193.
(20) Dementin, S., Leroux, F., Cournac, L., Lacey, A. L. de, Volbeda, A., Léger, C., Burlat, B., Martinez, N., Champ, S., Martin, L., Sanganas, O., Haumann, M., Fernández, V. M., Guigliarelli, B., Fontecilla-Camps, J. C., and Rousset, M. (2009) Introduction of methionines in the gas channel makes [NiFe] hydrogenase aero-tolerant. *J. Am. Chem. Soc. 131*, 10156−10164.
(21) Dance, I. (2012) The controlled relay of multiple protons required at the active site of nitrogenase. *Dalton Trans. 41*, 7647−7659.
(22) Seefeldt, L. C., Dance, I. G., and Dean, D. R. (2004) Substrate interactions with nitrogenase: Fe versus Mo. *Biochemistry 43*, 1401−1409.
(23) Cohen, J., Kim, K., Posewitz, M., Ghirardi, M. L., Schulten, K., Seibert, M., and King, P. (2005) Molecular dynamics and experimental investigation of H_2 and O_2 diffusion in [Fe]-hydrogenase. *Biochem. Soc. Trans. 33*, 80−82.
(24) Wang, P., and Blumberger, J. (2012) Mechanistic insight into the blocking of CO diffusion in [NiFe]-hydrogenase mutants through multiscale simulation. *Proc. Natl. Acad. Sci. U.S.A. 109*, 6399−6404.
(25) Wang, P., Best, R. B., and Blumberger, J. (2011) A microscopic model for gas diffusion dynamics in a [NiFe]-hydrogenase. *Phys. Chem. Chem. Phys. 13*, 7708−7719.
(26) Li, H., Robertson, A. D., and Jensen, J. H. (2005) Very fast empirical prediction and rationalization of protein pK_a values. *Proteins 61*, 704−721.
(27) Duan, Y., Wu, C., Chowdhury, S., Lee, M. C., Xiong, G., Zhang, W., Yang, R., Cieplak, P., Luo, R., Lee, T., Caldwell, J., Wang, J., and Kollman, P. (2003) A point-charge force field for molecular mechanics simulations of proteins based on condensed-phase quantum mechanical calculations. *J. Comput. Chem. 24*, 1999−2012.
(28) Price, D. J., and Brooks, C. L., 3rd (2004) A modified TIP3P water potential for simulation with Ewald summation. *J. Chem. Phys. 121*, 10096−10103.
(29) Wang, J., Wolf, R. M., Caldwell, J. W., Kollman, P. A., and Case, D. A. (2004) Development and testing of a general amber force field. *J. Comput. Chem. 25*, 1157−1174.
(30) Zeng, J., Duan, L., Zhang, J. Z., and Mei, Y. (2013) A numerically stable restrained electrostatic potential charge fitting method. *J. Comput. Chem. 34*, 847−853.
(31) Godbout, N., Salahub, D. R., Andzelm, J., and Wimmer, E. (1992) Optimization of Gaussian-type basis sets for local spin density functional calculations. Part I. Boron through neon, optimization technique and validation. *Can. J. Chem. 70*, 560−571.
(32) Smith, D. M. A., Xiong, Y., Straatsma, T. P., Rosso, K. M., and Squier, T. C. (2012) Force-field development and molecular dynamics of [NiFe] hydrogenase. *J. Chem. Theory Comput. 8*, 2103−2114.
(33) McDowell, S. A. C. (2003) Blue-shifting hydrogen bonding in N_2···HKrF. *J. Chem. Phys. 118*, 7283−7287.
(34) Lindahl, E., Hess, B., and van der Spoel, D. (2001) GROMACS 3.0: A package for molecular simulation and trajectory analysis. *J. Mol. Model. 7*, 306−317.
(35) Berendsen, H. J. C., Postma, J. P. M., van Gunsteren, W. F., DiNola, A., and Haak, J. R. (1984) Molecular dynamics with coupling to an external bath. *J. Chem. Phys. 81*, 3684−3690.
(36) Cheng, A., and Merz, K. M. (1996) Application of the Nosé−Hoover chain algorithm to the study of protein dynamics. *J. Phys. Chem. 100*, 1927−1937.
(37) Parrinello, M., and Rahman, A. (1981) Polymorphic transitions in single crystals: A new molecular dynamics method. *J. Appl. Phys. 52*, 7182−7190.
(38) Hess, B. (2008) P-LINCS: A parallel linear constraint solver for molecular simulation. *J. Chem. Theory Comput. 4*, 116−122.
(39) Ho, B. K., and Gruswitz, F. (2008) HOLLOW: Generating accurate representations of channel and interior surfaces in molecular structures. *BMC Struct. Biol. 8*, 49−54.
(40) Humphrey, W., Dalke, A., and Schulten, K. (1996) VMD: Visual molecular dynamics. *J. Mol. Graphics 14*, 33−38.
(41) Kumar, S., Rosenberg, J., Bouzida, D., Swendsen, R., and Kollman, P. (1992) The weighted histogram analysis method for free-energy calculations on biomolecules. I. The method. *J. Comput. Chem. 13*, 1011−1021.
(42) Hub, J. S., de Groot, B. L., and van der Spoel, D. (2010) g_wham−A free weighted histogram analysis implementation including robust error and autocorrelation estimates. *J. Chem. Theory Comput. 6*, 3713−3720.
(43) Khavrutskii, I. V., Dzubiella, J., and McCammon, J. A. (2008) Computing accurate potentials of mean force in electrolyte solutions with the generalized gradient-augmented harmonic Fourier beads method. *J. Chem. Phys. 128*, 044106-1−044106-13.
(44) Hess, B. (2002) Convergence of sampling in protein simulations. *Phys. Rev. E. 65*, 031910-1−031910-10.
(45) Yang, Z.-Y., Dean, D. R., and Seefeldt, L. C. (2011) Molybdenum nitrogenase catalyzes the reduction and coupling of CO to form hydrocarbons. *J. Biol. Chem. 286*, 19417−19421.
(46) Mayer, S. M., Niehaus, W. G., and Dean, D. R. (2002) Reduction of short chain alkynes by a nitrogenase α-70^{Ala}-substituted MoFe protein. *Dalton Trans.*, 802−807.
(47) Lee, H.-I., Igarashi, R. Y., Laryukhin, M., Doan, P. E., Dos Santos, P. C., Dean, D. R., Seefeldt, L. C., and Hoffman, B. M. (2004) An organometallic intermediate during alkyne reduction by nitrogenase. *J. Am. Chem. Soc. 126*, 9563−9569.
(48) Yang, Z.-Y., Moure, V. R., Dean, D. R., and Seefeldt, L. C. (2012) Carbon dioxide reduction to methane and coupling with acetylene to form propylene catalyzed by remodeled nitrogenase. *Proc. Natl. Acad. Sci. U.S.A. 109*, 19644−19648.
(49) Sarma, R., Barney, B. M., Keable, S., Dean, D. R., Seefeldt, L. C., and Peters, J. W. (2010) Insights into substrate binding at FeMo-cofactor in nitrogenase from the structure of an alpha-70^{Ile} MoFe protein variant. *J. Inorg. Biochem. 104*, 385−389.
(50) Schindelin, H., Kisker, C., Schlessman, J. L., Howard, J. B., and Rees, D. C. (1997) Structure of ADP·AlF_4^--stabilized nitrogenase complex and its implications for signal transduction. *Nature 387*, 370−376.

(51) Tezcan, F. A., Kaiser, J. T., Mustafi, D., Walton, M. Y., Howard, J. B., and Rees, D. C. (2005) Nitrogenase complexes: Multiple docking sites for a nucleotide switch protein. *Science 309*, 1377−1380.
(52) Hoffman, B. M., Lukoyanov, D., Dean, D. R., and Seefeldt, L. C. (2013) Nitrogenase: A draft mechanism. *Acc. Chem. Res. 46*, 587−595.
(53) Dos Santos, P. C., Igarashi, R. Y., Lee, H.-I., Hoffman, B. M., Seefeldt, L. C., and Dean, D. R. (2005) Substrate interactions with the nitrogenase active site. *Acc. Chem. Res. 38*, 208−214.
(54) Dilworth, M. J., Fisher, K., Kim, C.-H., and Newton, W. E. (1998) Effects on substrate reduction of substitution of histidine-195 by glutamine in the α-subunit of the MoFe protein of *Azotobacter vinelandii* nitrogenase. *Biochemistry 37*, 17495−17505.
(55) Dance, I. (2013) A molecular pathway for the egress of ammonia produced by nitrogenase. *Sci. Rep. 3*, 3237-1−3237-9.